Robotica (2012) volume 30, pp. 449–456. © Cambridge University Press 2011
doi:10.1017/S0263574711000646

Design and analysis of CICABOT: a novel translational parallel manipulator based on two 5-bar mechanisms

M. F. Ruiz-Torres, E. Castillo-Castaneda* and J. A. Briones-Leon

Centro de Investigacion en Ciencia Aplicada y Tecnologia Avanzada, Instituto Politecnico Nacional, Cerro Blanco 141, Colinas del Cimatario, Queretaro, Mexico

(Received in Final Form: May 31, 2011; accepted May 26, 2011. First published online: July 21, 2011)

SUMMARY

This work presents the CICABOT, a novel 3-DOF translational parallel manipulator (TPM) with large workspace. The manipulator consists of two 5-bar mechanisms connected by two prismatic joints; the moving platform is on the union of these prismatic joints; each 5-bar mechanism has two legs. The mobility of the proposed mechanism, based on Gogu approach, is also presented. The inverse and direct kinematics are solved from geometric analysis. The manipulator's Jacobian is developed from the vector equation of the robot legs; the singularities can be easily derived from Jacobian matrix. The manipulator workspace is determined from analysis of a 5-bar mechanism; the resulting workspace is the intersection of two hollow cylinders that is much larger than other TPM with similar dimensions.

KEYWORDS: Parallel manipulators; Translational parallel manipulator; Mobility analysis; 5-bar mechanism; Robot workspace.

1. Introduction

Parallel robots have become a very interesting option in the development of industrial applications due to the advantages that these mechanisms present compared with the conventional serial robots. For machining applications, such as milling and drilling, a 3-DOF manipulator is very suitable since it can be considerably lighter, making it possible to add additional DOF through a mechanism with independent actuators.[1–3] On the other hand, manipulation tasks often require high precision and very high speed positioning, so the parallel robots have been successfully applied in this type of task.[4–8] However, there are disadvantages that limit its use, such as the reduced working space and the existence of multiple singular configurations. There are several mechanisms, which are variants or combinations of parallel manipulators, seeking to the following: optimize workspace, increase stiffness, reduce the number of singularities, or simply facilitate analysis. A translational parallel manipulator (TPM) is a 3-DOF parallel mechanism whose output link, called mobile platform, can achieve three independent orthogonal translational motions with respect to the fixed base.

* Corresponding author. E-mail: ecastilloca@ipn.mx

The Orthoglide[9] is a variant of TPM developed in ref. [6], in which the workspace is optimized by a convenient location of legs and actuators. Another variant is the H4 developed in ref. [5]; the manipulator has a leg adding an extra DOF for rotation. The work described in ref. [10] presents a TPM that has legs with 5-DOF in each of them.

Gosselin and Angeles[11] have proposed kinematic analysis of some 3-DOFs parallel mechanisms. Synthesis and enumeration of possible 3-DOFs parallel mechanisms that can provide either translational or rotational DOFs have been extensively studied based on screw theory[12,13] and Lie group theory.[14–17] The work developed in ref. [18] presents a synthesis of 3-DOF pure TPMs, some novel examples, including doubly planar kinematic chains, are synthesized systematically. In ref. [14], a synthesis of orthogonal TPMs is developed using Lie group theory. Also, ref. [15] introduces four families of 3-DOF translational–rotational parallel mechanisms using Lie group theory.

Other designs that try to take advantage of the most basic mechanisms as 5-bar mechanism were developed in refs. [19, 20]. The aim of this work is to present the CICABOT, a novel TPM based on two 5-bar mechanisms developped at Centro de Investigacion en Ciencia Aplicada y Tecnologia Avanzada (CICATA), which is a research center of the Instituto Politecnico Nacional (IPN) in Mexico. The main advantages of our novel TPM are following: a very wide workspace, only limited by the size of the links; a very simple determination of inverse and direct kinematics; and the passive joints of the mechanism are mainly rotational ones, avoiding backlash and friction of spherical joints.

2. Design of the Mechanism

Figure 1(a) shows the mechanical structure of the proposed TPM. The fixed platform or base is a square frame; the mobile platform is composed of two prismatic joints located at 90° between them. The base is attached to the mobile platform through four legs. Figure 1(b) shows a side view of the proposed mechanism, one clearly observe one 5-bar mechanism. If this view of the mechanism rotates 90°, one can see an identical 5-bar mechanism. In ref. [21], a study on the optimization of the workspace of a 5-bar mechanism is presented.

As is shown in Fig. 2, each of the four legs *Gi* is composed of two links a_i, b_i; connected by rotational joints R_{i_2}. The link a_i is attached to the base by joint R_{i_1}. The legs G_1 and

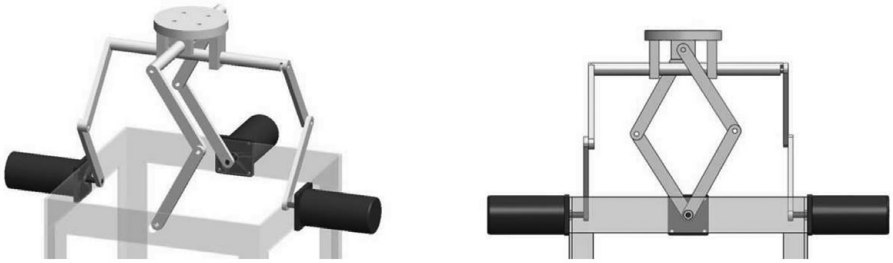

(a) (b)

Fig. 1. Schematic diagram of CICABOT: (a) 3D view and (b) side view.

G_2 are connected by c_{12} bar and two rotational joints R_{13} and R_{23}, thus forming a 5-bar mechanism. Similarly, G_3 and G_4 legs are connected by c_{34} bar and joints R_{33} and R_{34} forming a second 5-bar mechanism. The mobile platform is linked to the mechanism by two orthogonal prismatic joints Pr_1 and Pr_2 that slide through the bars c_{12} and c_{34} allowing, thus, only translational motion.

3. Mobility Analysis

Mobility or the degree of freedom is defined as the number of independent coordinates needed to define the configuration of a kinematic chain or mechanism.[22] Mobility (M) is used to verify the existence of a mechanism ($M > 0$), to indicate the number of independent parameters in the both kinematic and the dynamic models and to determine the number of inputs needed to drive the mechanism. A very wide review of methods on the calculation of the mobility is presented in ref. [23].

One of the most used formulas is the Grübler criterion proposed by Hunt,[24] which considers the number of links, number of joints, and types of joints incorporated in the mechanism.

An outstanding contribution to this formula is presented in ref. [6], where it is proposed to subtract the number of passive degrees of freedom from total degrees of freedom computed by Grübler criterion; it is possible to use this formula to determine the mobility of mechanisms with passive degrees of freedom as the Stewart platform. This and other important contributions were grouped into a formula known as CGK (Chebychev–Grübler–Kutzback). However, this formula is not applicable for all types of manipulators.[25] For example, in mechanisms that contain multiple closed loops, the mobility calculation is complicated because these closed loops cancel the mobility independence of some joints.

An innovative formula allowing the mobility calculation of serial and parallel mechanisms, with one or more closed loops in the sense of graph theory, is developed in ref. [26]. This method decomposes the mechanism in k closed loops and analyzes the motion restrictions in each closed loop, thus determines the overall mobility restrictions in the mechanism and consequently their mobility. The formula is defined as follows:

$$M = \sum_{i=1}^{p} f_i - r, \tag{1}$$

where M is the mechanism mobility, p is the total joints number, f_i is the mobility of ith joint, and r is the number of joint parameters that lose their independence in the mechanism after closing all the mechanism loops. The r variable is defined as

$$r = \sum_{i=1}^{k} S_{G_i} - S_F + r_l, \tag{2}$$

where k is the number of independent closed loops in the sense of graph theory, S_{G_i} is the connectivity of leg G_i when

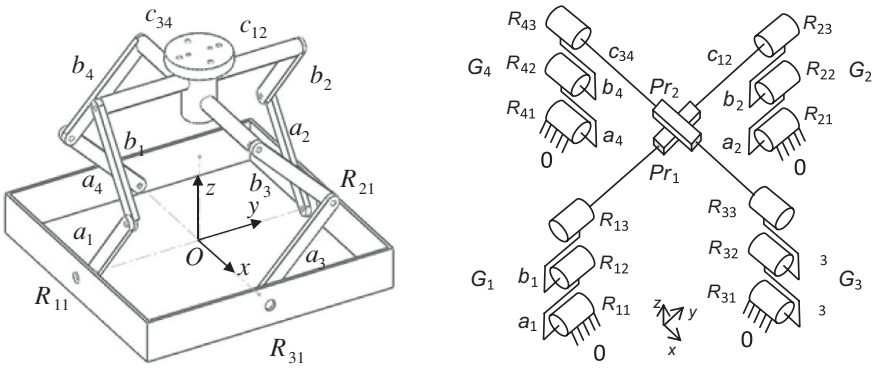

(a) (b)

Fig. 2. (a) Schematic diagram of CICABOT and (b) structure of the manipulator.

https://doi.org/10.1017/S0263574711000646 Published online by Cambridge University Press

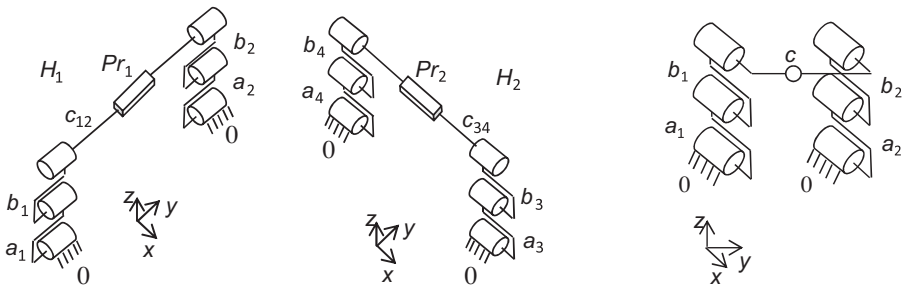

(a) **(b)** **(c)**

Fig. 3. (a) Legs G_1 and G_2, (b) legs G_3 and G_4, and (c) 5-bar mechanism H_1.

it is disconnected from the mechanism, S_F corresponds to the total connectivity of the mechanism, and r_l is the number of parameters that lose their independence in the ith closed loop.

Connectivity S_A of a simple open kinematic chain $A(1 - 2 - ... - n)$ is given by the connectivity between the final and reference links n and 1. Connectivity represents the number of independent finite displacements between the extreme links n and 1.

The number of joint parameters that lose their independence in the closed loop of the mechanism is given by the rank of the homogeneous linear set of velocity equations of the mechanism; those equations are not simple to calculate in the case of multiloop mechanisms. An alternative approach is to perform a symbolic calculation of the rank in an arbitrary position of the mechanism without indicating the numerical values of the joint variables and the geometric parameters. In such case, the variables S_{G_i} and S_F are defined as follows:

$$S_{G_i} = \dim(R_{G_i}),$$
$$S_F = \dim(R_F) = \dim(R_{G_1} \cap R_{G_2} \cap \cdots \cap R_{G_k}),$$

and

$$r_l = \sum_{i=1}^{k} r_l^{G_i}, \tag{3}$$

where R_F is the velocity vector of the mechanism, R_{Gi} is the velocity vector of leg G_i when it is disconnected from the mechanism, and $r_l^{G_i}$ is the number of parameters that lose their independence in the leg G_i.

Figure 3 shows the CICABOT decomposed in two 5-bar mechanisms. The legs G_1 and G_2 form a 5-bar mechanism, named H_1; the legs G_3 and G_4 form a second 5-bar mechanism, named H_2. From Gogu's definitions: $p = 14$ and $k = 2$. When H_1 and H_2 are disconnected (see Fig. 3), one can observe that the corresponding velocity vectors R_{H_1} and R_{H_2} related to mobile platform P are following: $R_{H_1} = \{v_x, v_y, v_z, \omega_y\}$ and $R_{H_2} = \{v_x, v_y, v_z, \omega_x\}$.

Then, the corresponding connectivity is $S_{H_1} = \dim(R_{H_1}) = S_{H_2} = \dim(R_{H_2}) = 4$. Therefore, the velocity vector of the mechanism is $R_{F_1} = R_{H_1} \cap R_{H_2} = v_x, v_y, v_z$; the corresponding connectivity is $S_{F_1} = \dim(R_{F_1}) = 3$.

To compute the number of parameters that lose their independence in the ith closed loop, each of the two 5-bar mechanisms should be disconnected (see Fig. 3c).

Disconnecting the legs G_1 and G_2 at point C, one can obtain the following corresponding velocity vectors and connectivity's:

$$R_{G1} = \{v_y, v_z, \omega_x\}; \quad S_{G1} = \dim(R_{G1}) = 3,$$

and

$$R_{G2} = \{v_y, v_z, \omega_x\}; \quad S_{G2} = \dim(R_{G2}) = 3.$$

Then, the mechanism velocity vector and connectivity are following:

$$R_{F2} = R_{G1} \cap R_{G2} = \{v_y, v_z, \omega_x\}; \quad S_{F2} = \dim(R_{F2}) = 3.$$

Substituting the values in Eqs. (2) and (3): $r_l^{H^1} = r_l^{H^2} = 3$, $r_l = 6$, and $r = 11$.

Therefore, substituting in Eq. (1), we obtain $M = 14 - -11 = 3$.

In conclusion, the mobility of the proposed novel TPM of this work is 3; it means that only three active joints are required. Thus, one of the legs does not have any active joint, in our case, the leg G_4 will be considered only as a support of leg G_3. It is not recommended to leave out the nonactuated leg since it contributes to increase robot rigidity giving an extra support leg to the mechanism.

4. Inverse and Direct Kinematics

4.1. Inverse kinematics

Figure 4 shows a simplified geometrical description of the novel TPM. The active joint variables are γ_i, with $i = 1, 2, 3$; the passive joints are γ_i; the legs positions are defined by distances d_i;h_1 is the distance between the top 5-bar mechanism and mobile platform; and h_2 is the distance between the two 5-bar mechanisms. The points P_1, P_2, P_3 are the final positions of legs 1,2,3, respectively; and the point P represents the final position of the mobile platform. From here, we use the following notation: $P_i = [p_{ix}, p_{iy}, p_{iz}]^t$.

From the geometrical representation in Fig. 4,

$$\overline{OA_i} + \overline{A_iB_i} + \overline{B_iP_i} = \overline{OP_i}. \tag{4}$$

https://doi.org/10.1017/S0263574711000646 Published online by Cambridge University Press

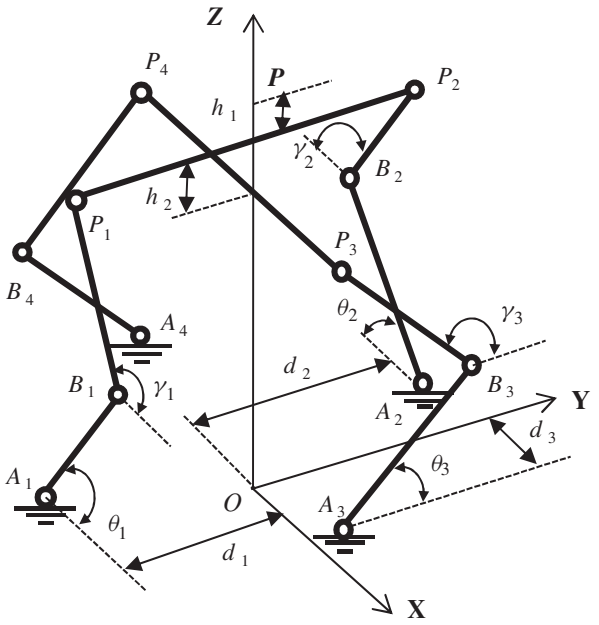

Fig. 4. Geometrical description of CICABOT.

Rewriting Eq. (4), we obtain Eqs. (5)–(7)

$$\begin{bmatrix} p_{1x} \\ p_{1y} \\ p_{1z} \end{bmatrix} = \begin{bmatrix} a_1 \cos\theta_1 + b_1 \cos\gamma_1 \\ -d_1 \\ a_1 \sin\theta_1 + b_1 \sin\gamma_1 \end{bmatrix}, \tag{5}$$

$$\begin{bmatrix} p_{2x} \\ p_{2y} \\ p_{2z} \end{bmatrix} = \begin{bmatrix} -a_2 \cos\theta_2 - b_2 \cos\gamma_2 \\ d_2 \\ a_2 \sin\theta_2 + b_2 \sin\gamma_2 \end{bmatrix}, \tag{6}$$

$$\begin{bmatrix} p_{3x} \\ p_{3y} \\ p_{3z} \end{bmatrix} = \begin{bmatrix} d_3 \\ a_3 \cos\theta_3 + b_3 \cos\gamma_3 \\ a_3 \sin\theta_3 + b_3 \sin\gamma_3 \end{bmatrix}. \tag{7}$$

The points P_1 and P_2 are collinear, while points A_2 and A_1 are collinear with respect to Y-axis, then

$$\begin{aligned} p_x &= p_{1x} = p_{2x}, \\ p_y &= p_{3y}, \\ p_z &= p_{1z} + h_1 = p_{2z} + h_1 = p_{3z} + h_1 + h_2. \end{aligned} \tag{8}$$

From Eq. (5),

$$(p_{1x} - a_1 \cos\theta_1)^2 + (p_{1z} - a_1 \sin\theta_1)^2 = (b_1 \cos\gamma_1)^2 + (b_1 \sin\gamma_1)^2. \tag{9}$$

Simplifying

$$p_{1x}^2 + p_{1z}^2 - 2a_1 p_{1x} \cos\theta_1 - 2a_1 p_{1z} \sin\theta_1 + a_1^2 - b_1^2 = 0. \tag{10}$$

Defining the following variables:

$$\begin{aligned} k_{11} &= -2a_1 p_{1x}, \\ k_{12} &= -2a_1 p_{1z}, \\ k_{13} &= p_{1x}^2 + p_{1z}^2 + a_1^2 - b_1^2. \end{aligned}$$

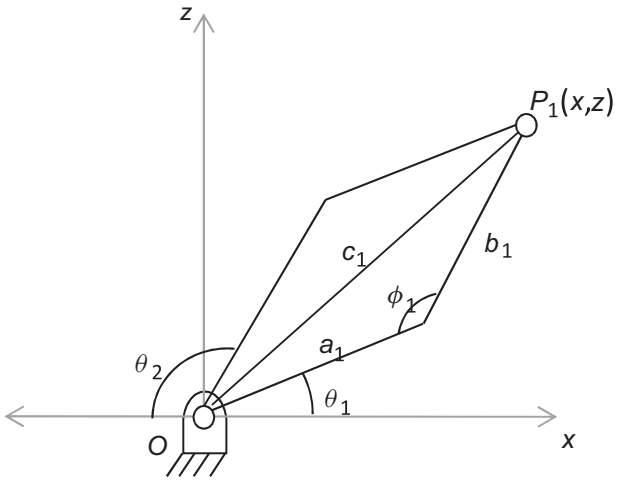

Fig. 5. Geometrical description of one 5-bar mechanism.

One can rewrite Eq. (10) as follows:

$$(k_{13} - k_{11}) \tan^2 \frac{\theta_1}{2} + 2k_{12} \tan \frac{\theta_1}{2} + k_{11} + k_{13} = 0.$$

Finally,

$$\theta_1 = 2 \tan^{-1} \left(\frac{-k_{12} \pm \sqrt{k_{12}^2 - k_{13}^2 + k_{11}^2}}{k_{13} - k_{11}} \right). \tag{11}$$

Likewise, Eqs. (6) and (7) result

$$\theta_2 = 2 \tan^{-1} \left(\frac{-k_{22} \pm \sqrt{k_{22}^2 - k_{23}^2 + k_{21}^2}}{k_{23} - k_{21}} \right), \tag{12}$$

$$\theta_3 = 2 \tan^{-1} \left(\frac{-k_{32} \pm \sqrt{k_{32}^2 - k_{33}^2 + k_{31}^2}}{k_{33} - k_{31}} \right), \tag{13}$$

where

$$\begin{aligned} k_{21} &= 2a_2 p_{2x}, \\ k_{22} &= -2a_2 p_{2z}, \\ k_{23} &= p_{2x}^2 + p_{2z}^2 + a_2^2 - b_2^2, \end{aligned}$$

and

$$\begin{aligned} k_{31} &= -2a_3 p_{3y}, \\ k_{32} &= -2a_3 p_{3z}, \\ k_{33} &= p_{3y}^2 + p_{3z}^2 + a_3^2 - b_3^2. \end{aligned}$$

4.2. Direct kinematics

The manipulator's direct kinematics is extremely simplified since each of the two 5-bar mechanisms moves only on a well-defined plane; the 5-bar mechanism named H_1 allows motions on plane X–Z; the 5-bar mechanism named H_2 allows motion on plane Y–Z.

https://doi.org/10.1017/S0263574711000646 Published online by Cambridge University Press

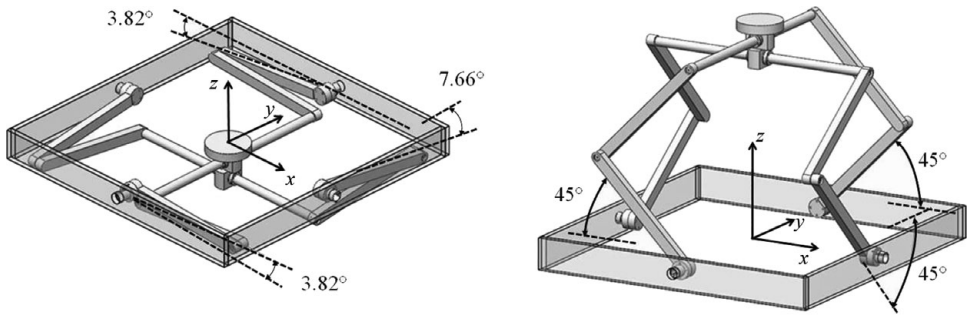

(a) (b)

Fig. 6. (a) First solution of inverse kinematics: $\theta_1 = -3.8°, \theta_2 = -3.8°, \theta_3 = -7.67°$ and second solution of direct kinematics: (b) $p_x = 0$ mm, $p_y = 88.15$ mm, $p_z = 464.26$ mm.

Figure 5 shows H_1 that is composed by legs G_1 and G_2 with two active joints θ_1 and θ_2. From Fig. 5,

$$c_1 = (a_1^2 + b_1^2 - 2a_1 b_1 \cos\phi_1)^{1/2}, \tag{14}$$

and

$$\phi_1 = \theta_1 + \theta_2. \tag{15}$$

Then,

$$\begin{aligned} p_{1x} &= c_1 \cos\left(\frac{180 + \theta_1 - \theta_2}{2}\right), \\ p_{1z} &= c_1 \sin\left(\frac{180 + \theta_1 - \theta_2}{2}\right). \end{aligned} \tag{16}$$

Rewriting Eq. (7) using the form of Eq. (10)

$$p_{3y}^2 + p_{3z}^2 - 2a_3 p_{3y} \cos\theta_3 - 2a_3 p_{3z} \sin\theta_3 + a_3^2 - b_3^2 = 0. \tag{17}$$

Substituting p_{3z}, from Eq. (8), in Eq. (17)

$$p_{3y}^2 + p_{3y}(-2a_3 \cos\theta_3) + (p_{1z} - h_2)^2 - 2a_3(p_{1z} - h_2) \sin\theta_3 + a_3^2 - b_3^2 = 0$$

gives

$$p_{3y} = \frac{-m_2 \pm \sqrt{m_2^2 - 4m_1 m_3}}{2m_1}, \tag{18}$$

where

$$\begin{aligned} m_1 &= 1, \\ m_2 &= -2a_3 \cos\theta_3, \\ m_3 &= (p_{1z} - h_2)^2 - 2a_3(p_{1z} - h_2)\sin\theta_3 + a_3^2 - b_3^2. \end{aligned}$$

Therefore, the manipulator's direct kinematics is defined by Eqs. (8), (16), and (18).

For example, given $a_i = b_i = 300$ mm, and $h_1 = h_2 = 40$ mm:

(1) Inverse kinematics, given $p_x = p_y = p_z = 0$, has two solutions:
First solution: $\theta_1 = -3.8°, \theta_2 = -3.8°, \theta_3 = -7.67°$,
Second solution: $\theta_1 = -176.18°, \theta_2 = -176.18°, \theta_3 = -172.34°$.

(2) Direct kinematics, given $\theta_1 = \theta_2 = \theta_3 = 45°$, has two solutions:
First solution: $p_x = 0$ mm, $p_y = 333.11$ mm, $p_z = 464.26$ mm,
Second solution: $p_x = 0$ mm, $p_y = 88.15$ mm, $p_z = 464.26$ mm.

Figure 6 shows the configurations corresponding to the first solution of inverse kinematics (see Fig. 6a), and second solution of direct kinematics (see Fig. 6b).

5. Manipulator's Jacobian

It is possible to determine the manipulator's Jacobian from joint velocities $[\dot\theta_1, \dot\theta_2, \dot\theta_2]$ and mobile platform velocities $V_p = [V_x, V_y, V_z]^t$, as is presented in ref. [26]. From Eq. (4), the velocity of the mobile platform can be derived as

$$V_p = \omega_{1i} \times A_i + \omega_{2i} \times B_i. \tag{19}$$

Premultypling by B_i

$$B_i \cdot V_p = \omega_{1i} \cdot (A_i \times B_i), \tag{20}$$

where for leg 1,

$$A_1 = \begin{bmatrix} a_1 \cos\theta_1 \\ 0 \\ a_1 \sin\theta_1 \end{bmatrix}; \quad B_1 = \begin{bmatrix} b_1 \cos\gamma_1 \\ 0 \\ b_1 \sin\gamma_1 \end{bmatrix};$$

$$\omega_{11} = \begin{bmatrix} 0 \\ -\dot\theta_1 \\ 0 \end{bmatrix}.$$

For leg 2,

$$A_2 = \begin{bmatrix} -a_2 \cos\theta_2 \\ 0 \\ a_2 \sin\theta_2 \end{bmatrix}; \quad B_2 = \begin{bmatrix} -b_2 \cos\gamma_2 \\ 0 \\ b_2 \sin\gamma_2 \end{bmatrix};$$

$$\omega_{12} = \begin{bmatrix} 0 \\ \dot\theta_2 \\ 0 \end{bmatrix}.$$

https://doi.org/10.1017/S0263574711000646 Published online by Cambridge University Press

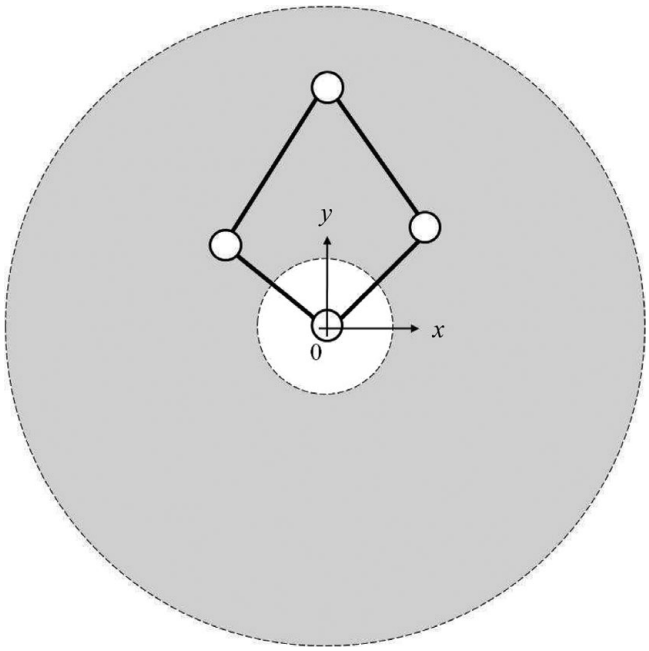

Fig. 7. The workspace of a typical 5-bar mechanism.

For leg 3,

$$A_3 = \begin{bmatrix} 0 \\ a_3 \cos\theta_3 \\ a_3 \sin\theta_3 \end{bmatrix}; \quad B_3 = \begin{bmatrix} 0 \\ b_3 \cos\gamma_3 \\ b_3 \sin\gamma_3 \end{bmatrix}; \quad \omega_{13} = \begin{bmatrix} \dot{\theta}_3 \\ 0 \\ 0 \end{bmatrix}.$$

Applying Eq. (20) for each leg,

$$(b_1 \cos\gamma_1)V_x + (b_1 \sin\gamma_1)V_z = ((a_1 \sin\theta_1)(b_1 \cos\gamma_1) - (a_1 \cos\theta_1)(b_1 \sin\gamma_1))(-\dot{\theta}_1),$$

$$(-b_2 \cos\gamma_2)V_x + (b_2 \sin\gamma_2)V_z = ((a_2 \cos\theta_2)(b_2 \sin\gamma_2) - (a_2 \sin\theta_2)(b_2 \cos\gamma_2))(\dot{\theta}_2),$$

$$(b_3 \cos\gamma_3)V_y + (b_3 \sin\gamma_3)V_z = ((a_3 \cos\theta_3)(b_3 \sin\gamma_3) - (a_3 \sin\theta_3)(b_3 \cos\gamma_3))(\dot{\theta}_3).$$

Rearranging the above equations in matrix form, we obtain

$$J_x V_p + J_\theta \dot{\theta} = 0, \tag{21}$$

where

$$J_x = \begin{bmatrix} b_1 \cos\gamma_1 & 0 & b_1 \sin\gamma_1 \\ -b_2 \cos\gamma_2 & 0 & b_2 \sin\gamma_2 \\ 0 & b_3 \cos\gamma_3 & b_3 \sin\gamma_3 \end{bmatrix};$$

$$J_\theta = \begin{bmatrix} J_{\theta 11} & 0 & 0 \\ 0 & J_{\theta 22} & 0 \\ 0 & 0 & J_{\theta 33} \end{bmatrix}$$

are the manipulator's Jacobian matrixes, with

$$J_{\theta 11} = (a_1 \cos\theta_1)b_1 \cos\gamma_1 - (a_1 \sin\theta_1)b_1 \cos\gamma_1,$$
$$J_{\theta 22} = (a_2 \cos\theta_2)b_2 \cos\gamma_2 - (a_2 \sin\theta_2)b_2 \cos\gamma_2,$$
$$J_{\theta 33} = (a_3 \cos\theta_3)b_3 \cos\gamma_3 - (a_3 \sin\theta_3)b_3 \cos\gamma_3.$$

The manipulator's singularities can be easily found from J_x and J_θ matrix.

6. Workspace

The manipulator's workspace can be determined from ref. [21] that presents an optimum design of a 5-bar mechanism. The corresponding workspace is ring shaped as is shown in Fig. 7.

In the case of the TPM presented in this paper, composed by two 5-bar mechanisms, the resulting workspace is the intersection of two hollow cylinders, shifted by a distance h_2. The radius of each cylinder is $l_1 < (a_1 + b_1)$ and $l_3 < (a_3 + b_3)$; theirs lengths are defined by c_{12} and c_{34}, respectively

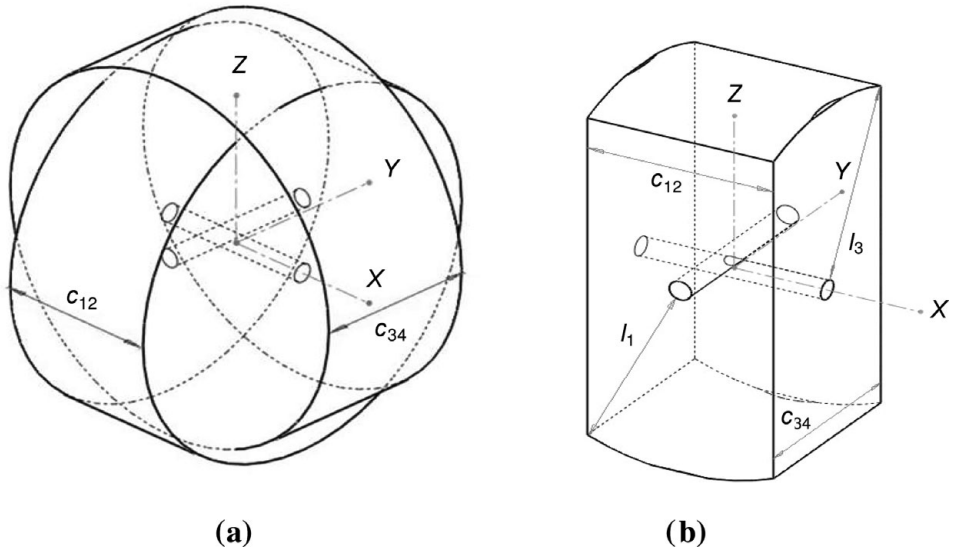

(a) **(b)**

Fig. 8. Workspace shape: (a) intersection of two cylinders and (b) resulting workspace.

https://doi.org/10.1017/S0263574711000646 Published online by Cambridge University Press

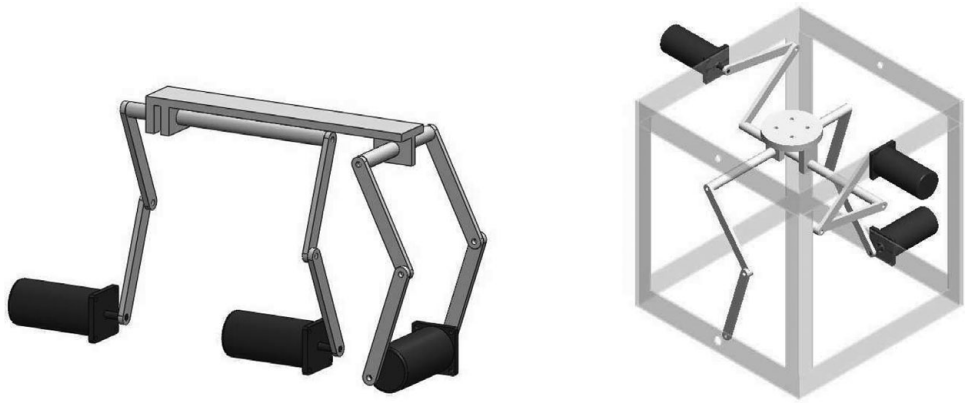

Fig. 9. Two different configurations of CICABOT using two 5-bar mechanisms.

(see Fig. 8a). One can see (Fig. 8b) that the geometry of the workspace is very close to a rectangle, so the volume of work space, in theory, is much higher than in other translational parallel mechanisms, where the workspace is close to a semicircle.

7. Conclusions

We designed a translational parallel robot of novel structure with a large workspace, consisting of two 5-bar mechanisms coupled with prismatic joints. The mobility analysis of the mechanism was performed using the method proposed

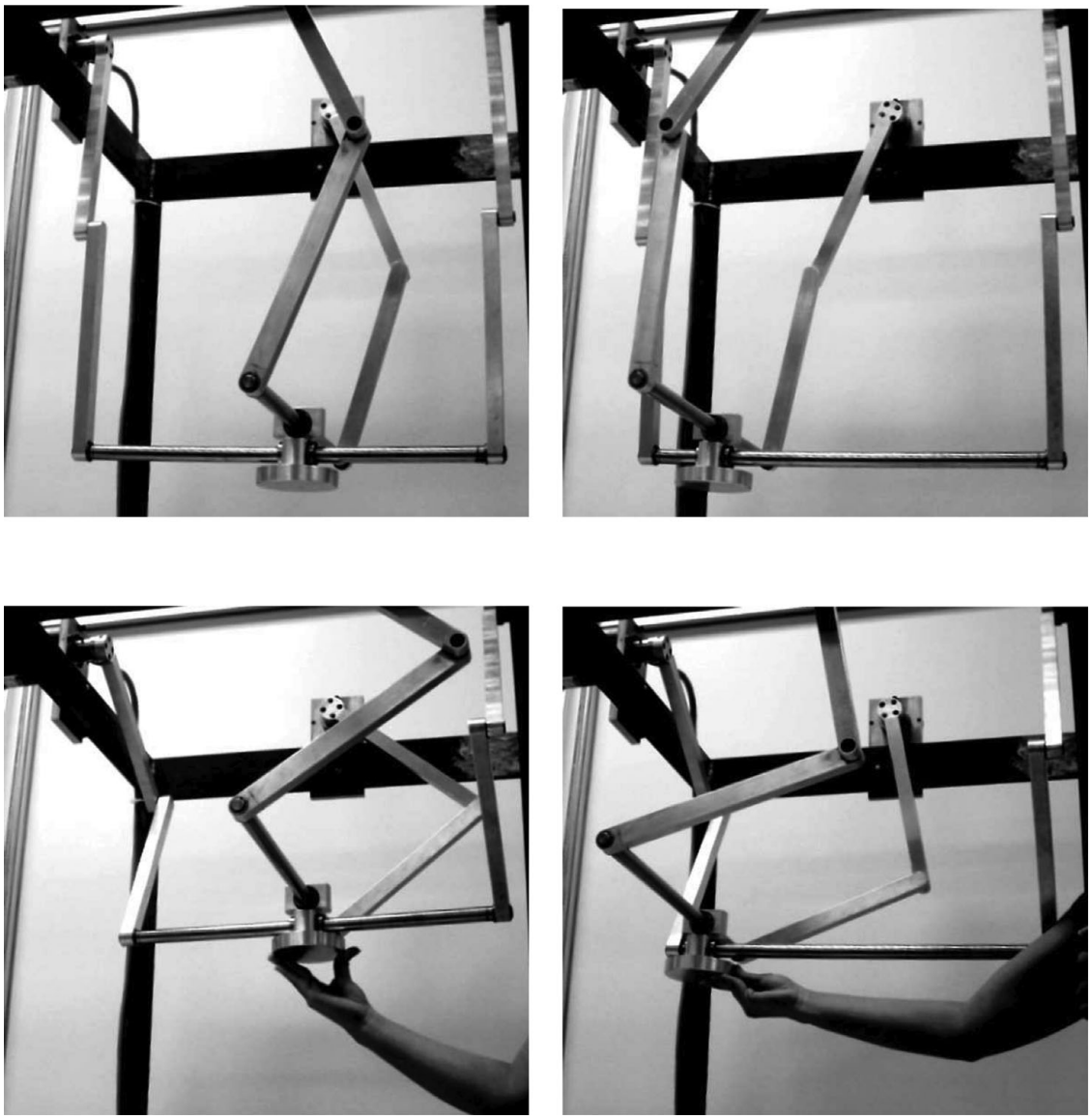

Fig. 10. Several poses of the first prototype of CICABOT.

https://doi.org/10.1017/S0263574711000646 Published online by Cambridge University Press

by Gogu.[26] This method determines mobility in a clear and accurate way for any type of mechanism, unlike other methods that are not valid for mechanisms with closed loops. Thanks to the decoupling of the two 5-bar mechanisms, the inverse and direct kinematics are solved very simply by geometrical considerations. The workspace can be considered as a rectangle whose dimensions are determined according to the lengths of the links. It was not necessary to apply advanced algorithms to calculate the workspace due to the simplicity of the geometric structure of the manipulator.

It is expected that the orthogonal layout of the two 5-bar mechanisms, which form the CICABOT help to improve rigidity, compared to that presented in the conventional 5-bar mechanisms. In addition, the four-point support of the CICABOT do provide a more stable structure than the classic three-point support of the parallel robot with 3-DOF, as for example the Delta robot.

The prismatic joint that connects the two 5-bar mechanisms should include a ball bearing to not reduce the stiffness of the mechanism. Also, all rotational passive joints are of the needle bearing type. On the other hand, the servomotors used as active rotational joints have high-speed reducers (120:1). This makes the complex dynamics of the robot is not reflected in the servomotors and therefore not reflected at the level of control algorithms. The use of counterweights or springs on opposite sides of the links a_i increases the payload of the robot.

It is possible to define new and original configurations of the manipulator depending of the 5-bar mechanism connection, such as shown in Fig. 9. Figure 10 shows some pictures of the first prototype of CICABOT in different poses; links are made in aluminum and prismatic joints are made in stainless steel with needle bearings.

Acknowledgments

This work was supported by the Instituto de Ciencia y Tecnologia del Distrito Federal (ICYT-DF), Ciudad de Mexico, project PIFUTP08-159.

References

1. T. J. Lindem and P. A. S. Charles, "Octahedral machine with a hexapodal triangular servostrut section," USA Patent 5401128 (1995).
2. T. Toyama, Y. Yamakawa and H. Susuki, "Machine tool having parallel structure," USA Patent 5715729 (1998).
3. C. L. Yau, "Systems and methods employing a rotary track for machining and manufacturing," USA Patent 6196081 (2001).
4. R. Clavel, "Device for the movement and positionin of an element in space," USA Patent 4976582 (1990).
5. F. Pierrot, O. Company, T. Shibukawa and K. Morita, "Four-degree-of-freedom parallel robot," USA Patent 6516681 (2003).
6. L. W. Tsai, "Multi-degree of freedom mechanism for machine tools and the like," USA Patent 5656905 (1997).
7. P. C. Sheldon, Six Axis Machine Tool, USA Patent 5388935 (1995).
8. T. Huang, Z. X. Li, M. Li, D. G. Chetwynd and C. M. Gosselin. "Conceptual design and dimensional synthesis of a novel 2-DOF translational parallel robot for pick-and-place operations," *J. Mech. Des.* **126**(5), 449–455 (2004).
9. D. Chablat and P. Wenger, "Architecture optimization of a 3-DOF translational parallel mechanism for machining applications, the orthoglide," *IEEE Trans. Robot. Autom.* **19**, 403–410 (2003).
10. M. Ruggiu, "Kinematics analysis of the CUR translational manipulator," *Mech. Mach. Theory* **43**, 1087–1098 (2008).
11. C. M. Gosselin and J. Angeles, "The optimum kinematic design of a spherical three-degree-of-freedom parallel manipulator," *J. Mech. Transm. Autom. Des.* **111**, 202–207 (1989).
12. X. Kong and C. M. Gosselin, "Type synthesis of 3-DOF spherical parallel manipulators based on screw theory," *ASME J. Mech. Des.* **126**, 101–108 (2004).
13. X. Kong and C. M. Gosselin, "Type synthesis of 3-DOF translational parallel manipulators based on screw theory," *ASME J. Mech. Des.* **126**, 83–92 (2004).
14. J. Yu, J. S. Dai, S. Bi and G. Zong, "Numeration and type synthesis of 3-DOF orthogonal translational parallel manipulators," *Prog. Nat. Sci.* **18**, 563–574 (2008).
15. S. Refaat, J. M. Hervé, S. Nahavandi and H. Trinh, "Asymmetrical three-DOFs rotational-translational parallel-kinematics mechanisms based on Lie group theory," *Eur. J. Mech. A* **25**, 550–558 (2006).
16. J. M. Hervé and F. Sparacino, "Structural Synthesis of Parallel Robots Generating Spatial Translation," *Proceedings of the 5th International Conference on Advanced Robotics*, Pisa, Italy (1991) vol. 1, pp. 803–813.
17. J. Angeles, "The qualitative synthesis of parallel manipulators," *ASME J. Mech. Des.* **126**, 617–624 (2004).
18. C. Lee and J. M. Hervé, "Translational parallel manipulators with doubly planar limbs," *Mech. Mach. Theory* **41**, 433–455 (2006).
19. L. J. Stocco and S. E. Salcudean, "Hybrid serial/parallel manipulator," USA Patent 6047610 (2000).
20. B. Monsarrat and C. Gosselin, "Workspace analysis and optimal design of a 3-Leg 6-DOF parallel platform mechanism," *IEEE Trans. Robot. Autom.* **19**, 954–966 (2003).
21. X. Liu, J. Wang and H. Zheng, "Optimum design of the 5R symmetrical parallel manipulator with surrounded and good-condition workspace," *Robot. Auton. Syst.* **54**, 221–233 (2006).
22. T. G. Ionescu, "Terminology for mechanisms and machine science," *Mech. Mach. Theory* **38** 597–901 (2003).
23. G. Gogu, "Mobility of mechanisms: A critical review," *Mech. Mach. Theory* **40**, 1068–1097 (2005).
24. K. Hunt, *Kinematic Geometry of Mechanisms* (Oxford University Press, Oxford, UK, 1978).
25. G. Gogu, "Chebychev–Grübler–Kutzbach's criterion for mobility calculation of multi-loop mechanisms revisited via theory of linear transformations," *Eur. J. Mech. A* **24**, 427–441 (2004).
26. G. Gogu, *Structural Synthesis of Parallel Robots, Part 1—Methodology* (Springer, The Netherlands, 2008).